

Cathodoluminescent Phosphor Light Sources
Excited by High Pulsed Excitation

By

CLAUDIO LOPEZ OSSES
THESIS

Submitted in partial satisfaction of the requirements for the degree of

MASTER OF SCIENCE

in

Electrical and Computer Engineering

in the

OFFICE OF GRADUATE STUDIES

of the

UNIVERSITY OF CALIFORNIA

DAVIS

Approved:

Charles Hunt, Chair

Diego Yankelevich

Weijian Yang

Committee in Charge

2021

Acknowledgement

I would like to express my gratitude and appreciation to my Master supervisor Professor Charles E. Hunt, for his support throughout my studies and research at UC Davis.

The completion of this study could not have been possible without the patience and encouragement of Elizabeth Jara Torres.

I would like to thank Professor Diego R. Yankelevich and Professor Weijian Yang for accepting to serve on my dissertation committee.

Many thanks to Muhammed Tan, Sushma Shrinivasan, Michael Wong, Jonathan Marrs and all other colleagues for their support during my studies and research in all forms. and to Mr. Bernard Vancil for his useful suggestions.

Table of Contents

Chapter 1

1.1 Literature review

1.1.1 Cathodoluminescence Phenomena.....	2
1.1.2 Phosphor Materials.....	3
1.1.3 Cathodoluminescence efficiency and saturation.....	4
1.1.4 Persistence.....	6
1.1.5 Cathodoluminescent Phosphor Light sources.....	7
1.1.6 High Voltage Pulse Supply.....	8
1.1.7 Flyback Transformer	10

1.2. Problem's Statement

1.2.1 Efficiency.....	11
1.2.2 Lifetime	12
1.2.3 High Voltage Pulsed Power Supply.....	12

Chapter 2

2.1 Cathodoluminescent Phosphor Light bulbs Vu1

2.2.1 Electron gun and set up of DC and Pulsed excitation.....	14
--	----

2.2 Design of High Voltage Pulsed Supply

2.2.1 Flyback Transformers Power Supply.....	16
2.2.2 Flyback converter.....	19
2.2.3 IC controller.....	20
2.2.4 Switching MOSFET.....	21

2.3 Flyback Transformer Simulation.....

22

2.4 Flyback series connection.....

24

Chapter 3

3.1 Pulsed Voltage Power Source Results.....

27

3.2 Pulsed and DC excitation driving the Vu1 light bulb	
3.2.1 Experimental results by using pulsed voltage excitation.....	28
3.2.2 Experimental results by using DC voltage excitation.....	32
3.3 Comparison	
3.3.1 Comparison of the results by using different Pulsed excitation.....	34
3.3.2 Comparison between different Pulsed and DC excitations	37
4 Conclusion and Future Work.....	37
5 References.....	39

Abstract

The efficiency and lifetime rate of the cathodoluminescence phosphors light bulbs were improved using pulsed voltage excitation. The experiments were focused on exciting phosphor materials by inputting pulsed voltages of 90, 500 and 1000 Hz instead of DC voltage excitation for phosphor light bulbs. This work also shows the design, construction, and implementation of a pulsed power supply based on flyback transformers to drive the cathodoluminescent phosphor light sources.

The improvements were measured and analyzed by comparing the temperature and luminance of results by using DC and different pulsed voltage excitation. The result of flyback pulsed power supply concludes to be a feasible power supply to obtain high voltages at low cost to drive the Vu1 phosphor light sources. The temperature and luminance results showed that driving phosphor sources by using pulsed excitation rather than direct current excitation improves the lifetime and efficiency.

List of Figures

Figure 1.1: Schematic representation of energies of processes in cathodoluminescence, A) back-scattered primary electrons, B) back-scattered primary electrons with some energy loss, C) low-velocity secondary electron emission, hv) luminescence emission.....	2
Figure 1.2: FIG. I. Models of luminescent transitions. (a) Direct recombination of a free electron and a hole (band-to-band transition); (b) transition of a free electron to an acceptor level (c) recombination transition of a donor electron with a free hole (d) transition between a donor and an acceptor (e) transition within a localized luminescent center.....	4
Figure 1.3: The CL intensity is plotted against the anode voltage V_a at a current density $I_e = 0.1 \text{ [mA/mm}^2\text{]}$ (A), and against the current density I_e at an voltage $V_a=10\text{KV}$ (B). The measurements were performed for ZnS:Cu:Al phosphors in a 19-inch CRT screen.....	5
Figure 1.4: buildup and decay of screen luminescence, the rise and fall of screen luminance under pulse excitation.....	6
Figure 1.5: Schematic of the Vu1 light bulb.....	7
Figure 1.6: Marx Generator.....	9
Figure 1.7: Basic flyback converter circuit.....	10
Figure 1.8: Experimentally obtained values for the peak near-bandgap CL intensity in ZnO:Li as a function of temperature	11
Figure 1.9: Ageing characteristics at various accelerating voltage on SrGa ₂ S ₄ :Ce ³⁺	12
Figure 2.1: Circuit design for DC excitation.....	15
Figure 2.2: Circuit design for Pulsed excitation.....	15
Figure 2.3: Picture of the electron gun in Vu1 light bulb.....	16
Figure 2.4: Diagram of the flyback transformer.....	17
Figure 2.5: Flyback - switching cycle DCM Mode.....	18
Figure 2.6: Flyback Transformer.....	20
Figure 2.7: IC controller using diodes.....	20
Figure 2.8: Turn-off of the power switch signal in the switch mode without the RC snubber.....	21
Figure 2.9: RC snubber circuit design.....	21
Figure 2.10: Circuit and results of pulsing power supply simulation, Top spice.....	23
Figure 2.11: Flyback converter series connection.....	24
Figure 3.1. Flyback Output Voltage.....	27

Figure 3.2: Stabilization time of Vu1 light source by using pulse excitation.....	28
Figure 3.3: Luminance and Temperature for different anode current and accelerating voltage of 15kV..	28
Figure 3.4: Data collected by using pulse excitation with a frequency of 90 Hz.....	29
Figure 3.5: Data collected by using pulse excitation with a frequency of 500Hz.....	30
Figure 3.6: Data collected by using pulse excitation with a frequency of 1 kHz.....	30
Figure 3.7: Stabilization time of the Vu1 light source by using DC excitation.....	31
Figure 3.8: Data collected by using DC excitation.....	32
Figure 3.9: Vu1 Temperature results by using different Pulsed excitations.....	33
Figure 3.10: Vu1 luminance results by using different Pulsed excitations.....	33
Figure 3.11: VU1 Temperature results using different Pulsed and Direct Current excitation.....	34
Figure 3.12: VU1 Luminance results using different Pulsed and Direct Current excitation.....	35
Figure 3.13: VU1 Luminance results ratio of Pulsed/DC excitation.....	36

List of Tables

Table 2.1: List of actives and passive components for flyback transformer simulation.....	22
Table 3.1: Values applied to the Vu1 light Bulb.....	28
Table 3.2: Values applied to the Vu1 light Bulb.....	32
Table 3.3: voltages applied to electron gun for DC excitation.....	33

Chapter 1

1.1 Literature review

In modern society, energy conservation is an ambition sought by various stakeholders. In the United States of America, light energy consumption is estimated at 10% of the total electricity consumed by the residential and commercial sectors, which translate into 7% of total electricity consumption in America [1]. Notably, the lighting industry in the United States of America is capped by policies and rules that strive to reduce energy consumption and contribute to environmental protection; therefore, it is essential to produce innovative products in the lighting market that comply with the policies of energy reduction and environmental protection.

In terms of the lighting market, there are five energy-efficient lighting technologies in the market, namely fluorescent, light-emitting diode (LED), infrared-reflecting halogen, Organic light-emitting diode (OLED), and High-intensity discharge (HID). However, each of these lighting technologies exhibits some disadvantages, which limit their functionality as energy-efficient lighting technologies. As an example, toxicity and poor color quality are limitations in fluorescent lamps. Similarly, LEDs have problems with thermal dissipation that contributes to a significant temperature rise, reducing the color quality and efficiency especially in large-area applications. Alternatively, infrared-reflecting halogens have a reduced lifetime and high heat dissipation. OLEDs have high cost, insufficient brightness, and reduced lifetime. The HID

technology has a high heat dissipation rate in addition to high glare, which is the dominant challenge of HID technology.

The facts as explained above, mandate the need to investigate other forms of lighting technology focusing on high efficiency, which will translate into reduced cost and environmental protection. In this work, A new cathodoluminescence phosphor light-source technology has been investigated [2,3,4,5].

1.1.1 Cathodoluminescence Phenomena

Phosphors are solid luminescent materials that emit photons when excited by an external energy source such as an electron beam (cathodoluminescence), UV light (photoluminescence), electric field, currents, chemical reaction, etc. In the event of cathodoluminescence (CL) emission, the occurrence results from the penetration of a primary electron beam into the phosphor that can be seen in Figure 1.1.

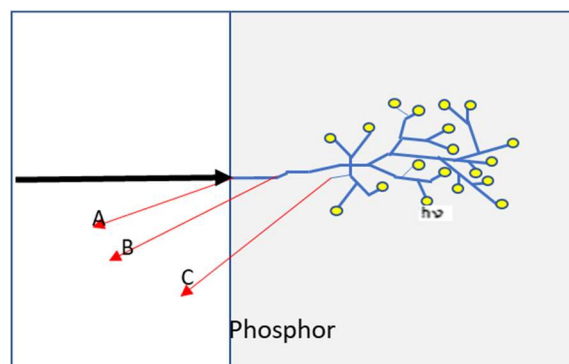


Figure 1.1: Schematic representation of energies of processes in cathodoluminescence
A) back-scattered primary electrons, B) back-scattered primary electrons with some energy loss, C) low-velocity secondary electron emission, $h\nu$) luminescence emission. [6]

Figure 1.1 shows an energetic electron accelerated by high voltage entering into a crystal. The impact produces hundreds of free electrons and holes along the path of the incident electron. The intensity of the light produced will depend on the energy available when the exciting secondary electrons return to their ground states via suitable radiative transitions, explained by the model of luminescent transitions of the phosphor material [6].

1.1.2 Phosphor materials

They are composed mainly of a host lattice which have a band gap around two or three electron volts and is transparent enough in the visible range to enable the transfer of visible light to the surface of the powder crystallites. The second component is the impurities that activate the crystal to luminesce, which are referred to as an activator. The activators will create localized energy levels in the bandgap, providing effective recombination paths for the excited electrons and holes. In practice, the primary properties of CL are characterized by intensity and color. These characteristics are determined by the nature of luminescence centers (activators) doped in host crystals.

Zinc sulfide can explain a simplified model mechanism of excitation. The unexcited state of the crystal is shown in Figure 1.2. The impurity state represents a level of the "activator" element, such as Cu and Ag activators in ZnS:Cu, Ag and ZnS:Ag, Cl phosphors. The activators will create localized energy levels in the bandgap, as represented by transitions (b), (c), and (d) in Fig. 1.2. These transitions, overwhelming the direct transition (a), emit light whose photon energy is smaller than the bandgap in accordance with the depths of these levels. [7,8,9]

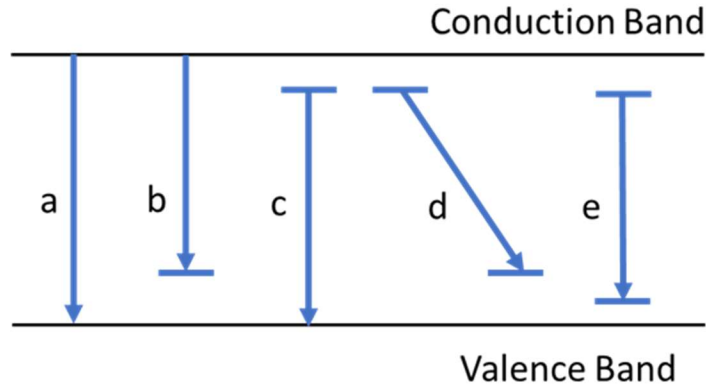


Figure 1.2: Models of luminescent transitions. (a) direct recombination of a free electron and a hole (band-to-band transition); (b) transition of a free electron to an acceptor level (c) recombination transition of a donor electron with a free hole (d) transition between a donor and an acceptor (e) transition within a localized luminescent center [7].

1.1.3 Cathodoluminescence efficiency and saturation

As illustrated in Figure 1.1, there are other losses than luminescence centers that affect the production of photons during the cathodoluminescence. The most significant losses correspond to the primary electrons by reflection and back scattering, accounting for 30% to 50% of the incident energy. For electrons that are not reflected, part of the energy is transformed on phonon scattering of the ‘hot’ secondary electrons, another goes to the lattice electrons and is not transmitted to the activators, then it will be lost in the form of heat. Consequently, the energy efficiency of the fluorescence must be less than 100%. The highest value reached in practice is about 20% [6,7].

Equation 1.1 is used to calculate the CL intensity, it is the relation of the energy W of electrons injected into a phosphor particle, with the multiplication of the anode voltage, and the electron beam density on the phosphor screen is the proportional constant [8].

$$W = k * V_a * I_e \quad \text{eq. 1.1}$$

The curves for the intensity of the light versus different excitations are shown in Figure 1.3. In the graph, the light intensity increases in direct proportion with voltage or current density, and the efficiency of the fluorescence decreases when the load is high. Eventually, the intensity will not increase by increasing the current density, in which case, the event is called saturation.

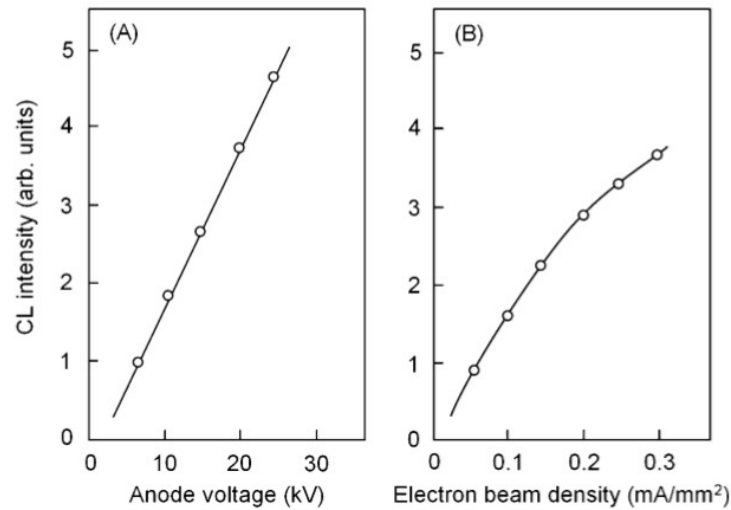


Figure 1.3: The CL intensity is against the anode voltage V_a at a current density $I_e = 0.1$ [mA/mm²] [mA/mm²] (A), and against the current density I_e at a voltage $V_a=10$ KV (B). The measurements were performed for ZnS:Cu:Al phosphors in a 19-inch CRT screen [8].

It is called saturation, when the proportionality between the light output and the intensity of the electron beam is disturbed. In most crystals, the electrons excited in saturation return to their original state without any emission because the excitation energy is converted into the lattice energy, i.e. heat.

There is another phenomenon affecting the proportionality between current density and the light output: owing to bombardment by the electrons, the fluorescent screen becomes heated, and above a specific critical temperature, the fluorescence of solids tends to decrease

rapidly with rising temperature, when that critical level is exceeded, the light output does not increase with the current at the same rate as it does in the case of lower temperatures [7].

1.1.4 Persistence

The persistence is the phosphors' characteristic that determines its ability to emit light for a time after the stimulus has been extinguished and the decay of phosphorescence as a function of time. Figure 1.4 shows a cathodoluminescence material that emits light after the end of the cathode excitation.

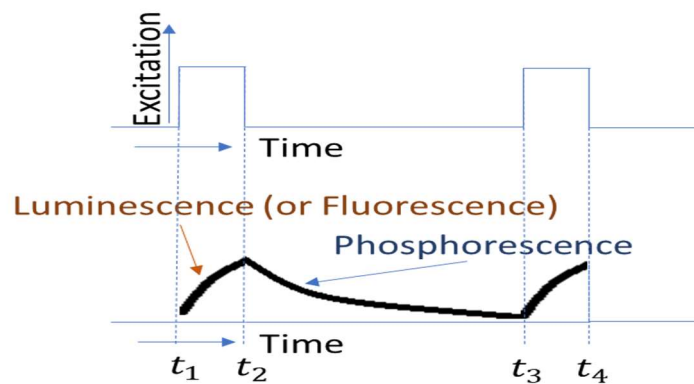


Figure 1.4: buildup and decay of screen luminescence, and the rise and fall of screen luminance under pulse excitation.

It is assumed that the electronic excitation of the screen is constant from time t_1 to t_2 , and off between time t_2 to t_3 . When the electrons strike the screen, the luminescence or fluorescence increases rapidly and follows the buildup curve that is characteristic of the phosphor. At t_2 , when the excitation is discontinued, the light output immediately begins to fall, and follows the characteristic phosphorescence decay of the phosphor [10].

One of the more popular equation to characterize the exponential is shown in equation 1.2.

$$I(t) = I_1 \exp\left(\frac{-t}{\tau_1}\right) + I_2 \exp\left(\frac{-t}{\tau_2}\right) \quad \text{eq. 1.2}$$

Where $I(t)$ represents the phosphorescent intensity at the time of the decay, I_1 and I_2 are two constants representing the rapid and slow initial luminescent intensity at $t=0$; τ_1 and τ_2 are parameters for the exponential components and determine the rapid and slow decay process.

1.1.5 Cathodoluminescent Phosphors Light Source

Figure 1.5 shows a schematic of the Vu1 light bulb. The components are a vacuum envelope, pumped using a getter, a cathode, which emits a “flood” of electrons uniformly accelerated toward the inner surface of the envelope upon which the CL phosphors are applied. The electron optics restrict the electrons to the phosphor layer, which has a reflective layer or conduction layer.

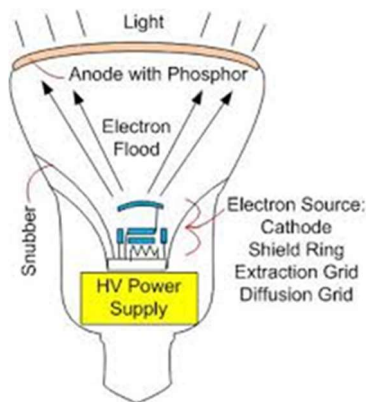


Figure 1.5: Schematic of the Vu1 light bulb

The power supply has high-voltage output and the total electron current is maintained such that the power density at the phosphor is lowly producing an efficient lamp [5].

1.1.6 High Voltage Pulse Supply.

A problem in phosphor lamp technologies is the range of voltage necessary to produce efficient brightness, for ray tubes CRT and FED, the brightness is around 70 cd/m^2 , in the case of television it should be between 200 and 300 cd/m^2 . However, to be used for light bulbs; the brightness should be at least 30000 cd/m^2 . The brightness can be produced in an efficiency manner by using the accelerating voltage above 10kV [11] which is known as medium voltage (MV). MV ranges have been used for a valve transmitter circuit, TV cathode ray tube, X-ray tube and other high voltage test equipment. Some of these MV supplies such as those used for radio transmitters or particle accelerators demand substantial currents, but for phosphors lamps it can be less than 1mA/cm^2 .

Phosphor lamps must use medium or high voltage, and the voltage to drive it can be provided principally in three forms: DC voltage, sinusoidal voltage, and pulsing voltage [3,4]. In case of pulsing voltage, many different topologies have been offering this range of voltage, one of them is the Marx Generator. Tammo Heeren et al., has worked with this circuit topology to micrometer size plasmas, or micro plasmas, used for pollution control, reduction, and prevention [12].

The Marx Generator consists of N parallel capacitors connected through resistors to a voltage V_0 . When the switches close simultaneously, capacitors become connected in series with a voltage of NV_0 across the load [12].

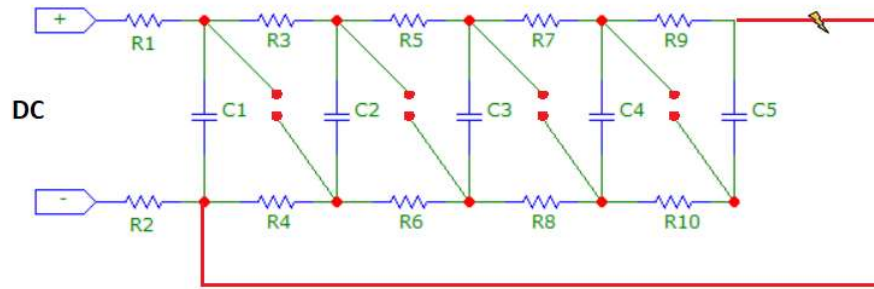


Figure 1.6: Marx Generator

Another circuit topology that can be used for MV and HV is a magnetic pulse compressor (MPC). Jaegu Choi et al. has worked on high power pulse generator using MPC; it has reached high repetitive operation of magnetic switches (MS) with low loss, it can be used for radar modulation, nuclear particle acceleration, and impulse testing for a long time. Pulse forming network (PFN) is a technique that can generate a good square shape pulse with fast rise and fall times and using Blumlein-type PFN (BPFN) helps reach the potential and pulse amplitude required [12].

Marx Generator, MPC, and other topologies such as pulse forming network can be used for MV or HV, but all of them present complexity, inflexibility, and inefficiency to be used in a small space such as regular light bulb.

1.1.7.- Flyback Transformer

One of the topologies used in phosphor lamps is the flyback power supply shown in Figure 1.7.

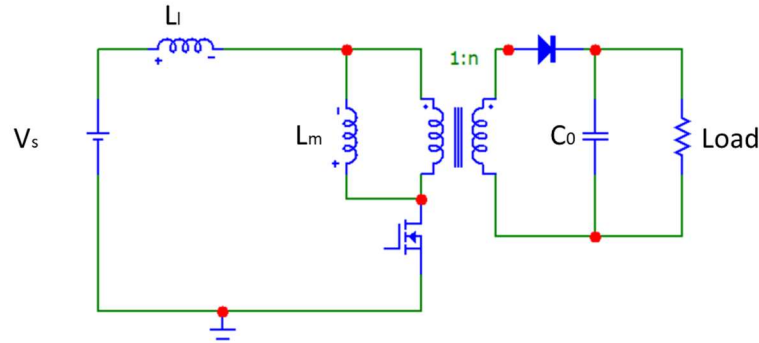


Figure 1.7: Basic flyback converter circuit

A flyback converter store energy from a source into a primary magnetizing inductance in the transformer when the switch is on and then transfers the stored energy to the load while the switch is off.

Some of the advantages of the flyback transformer are its isolation, lower voltage rate switches, the switch is in the off-state during the output pulse, high-voltage output with a low input dc voltage, low cost, and simple design [3,12].

Chang-hun lin et al. has been working in a pulsing power supply to drive FEL. In 2011 has proposed a pulse power supply operated in discontinuous conduction mode (DCM) for driving tubular field emission lamps (TFEL) by using the schematic shown in Figure 1.7. He concluded that the arcing caused by accumulating of excess charges in the phosphor layer is avoided with this configuration [3].

1.2. Problem's Statement

The pulsed cathodoluminescence considers the pulse as the excitation source to produce luminance in phosphor lamps instead of DC excitation. This thesis is focused on the construction and application of a pulsed voltage supply to increase the efficiency and lifetime rate described in the following subtopics.

1.2.1 Efficiency

Generally, the phosphor has a better lumen efficiency while excited by a higher voltage. However, the constant power or DC voltage driving will result in a temperature rise with corresponding efficiency loss. As can be seen in Figure 1.9, the temperature is directly related to the intensity of the phosphor lamps. It can be due to thermal quenching that can also cause saturation of luminescence at the high electron-beam current levels used in high-brightness [7,9]. In this work, a solution that considers the pulsed cathodoluminescence is proposed, the pulse method for driving the phosphor lamps considers a lower number of injected electrons in the material, offering rest time to lower the temperature.

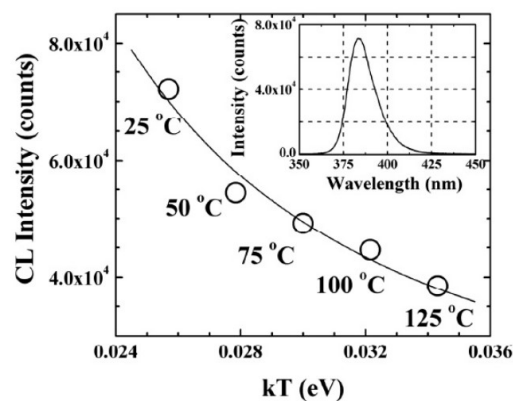


Figure 1.8: Experimentally obtained values for the peak near-bandgap CL intensity in ZnO:Li as a function of temperature [9].

1.2.2 Lifetime rate.

The lifetime rate of the phosphor screen is recognized as an issue in the cathodoluminescence process. The bombarding electrons behave as reducing agents and produce colloidal metal in the screen and other nonmetallic constituents often evaporating from it. The deterioration phenomena are not yet clear, but many of them are attributed to the prolonged electron bombardment called the electron burn. It can be seen in Figure 10 that the degree of burn decreases when the electron voltage increases [7,8,9,13]. This must be associated with the increase in the electron penetration into the phosphor and the consequent lowering of the excitation density per unit volume. The pulsed cathodoluminescence also offers a solution for this problem due to the injection of fewer electrons that impact the material.

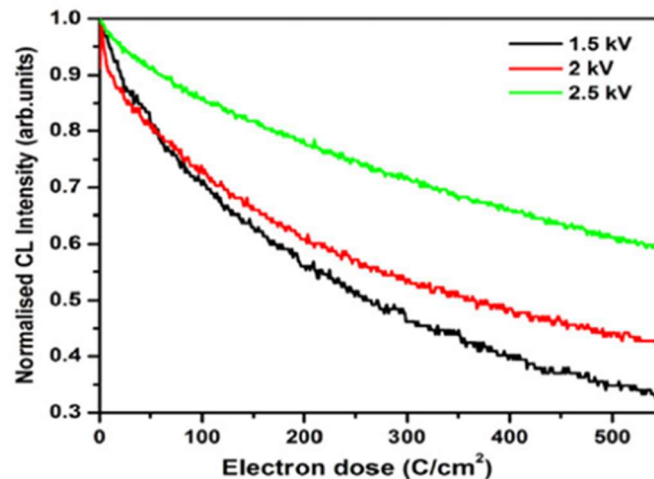


Figure 1.9: Aging characteristics at various accelerating voltage on $SrGa_2S_4:Ce^{3+}$ [13]

1.2.3 High Voltage Pulsed Power Supply

Another significant disadvantage of this technology is the high voltage requirement of the power supply. The voltage to drive the FEL's and phosphors lamp source can be provided principally in three forms: DC voltage, sinusoidal voltage, and pulsing voltage [3,4]. DC voltage

has been produced successfully, but the continuous excitation produces saturation in phosphor, decreasing the lifetime and using unnecessary power to excite the light. Sinusoidal voltage can be easily achieved, but its effective electric field will be too short, and the negative voltage will reduce the lifetime [3].

In this work, a flyback pulsed voltage power supply is designed, constructed, and implemented for driving phosphor lamps focusing on the increment of the lifetime rate and efficiency. The pulsing power supply will be implemented in commercial lamps provided by Vu1. As a part of the objective, this work will compare the results of DC voltage and pulsed voltage excitation in terms of luminance and temperature.

Chapter 2

Experimental Design and Modeling

This section explains the circuit's design and evaluate the DC and Pulsed excitation for driving the phosphor lamps. A high voltage pulsed power supply is designed, simulated, and built for voltage values around 4kV with around 1% duty cycle, with frequencies between 50-2kHz.

2.1 Cathodoluminescent phosphors Light bulbs

The experiments were performed on the Vu1 phosphor light bulbs excited by DC and Pulsed voltage. The format is the R-30 source which is used in standard residential dimmable downlight luminaires. The light source is composed of a vacuum envelope that contains a cathode that emits a "flood" of electrons, uniformly accelerated toward the inner surface of the envelope upon which the CL phosphors are applied. The CL phosphor lamp is manufactured and marketed exclusively by Vu1 Corporation [5]. A schematic of the light source is shown in the figure 1.5.

2.2.1 Electron gun and set up of DC and Pulsed excitation

The electron gun is a thermal field emission gun with a suppressor and an extractor electrode. The electrodes are circularly symmetric about the optical axis. The suppressor is negatively biased with respect to the cathode, while the extractor is positively biased.

There are 6 connectors in the Vu1 electronic supply; they are the heater, ground, V_{g1} , V_{g2} , and V_{g3} and the accelerating voltage. The current around 1A will go through the heater and increasing the temperature on the cathode, then the electrons can be extracted, suppressed and directed by the V_{g1} , V_{g2} , and V_{g3} voltages. The voltage between the anode and cathode called accelerating voltage will be higher than 10kV and located in the phosphor coated in the front surface.

The voltages for V_{g1} , V_{g2} , and V_{g3} are around 20, 100, 100 respectively for DC sources. The DC excitation is shown in Figure 2.1 and the pulse excitation is shown in Figure 2.2. Figure 2.3 shows a picture of the electron gun.

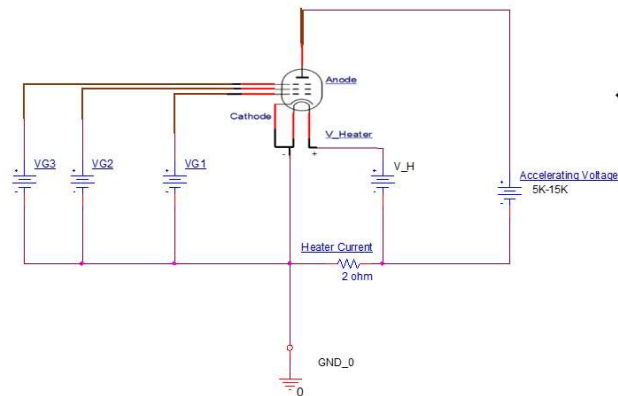


Figure 2.1: Circuit design for DC excitation

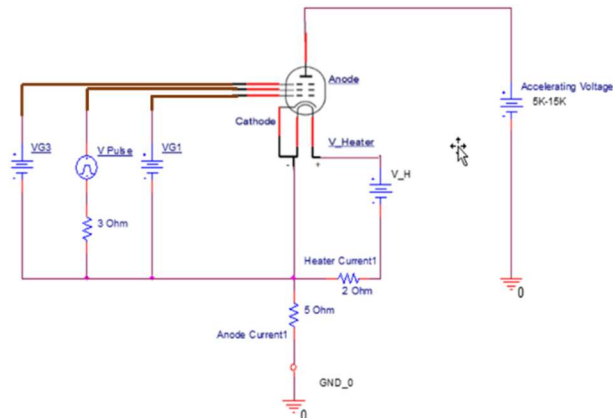


Figure 2.2: Circuit design for Pulsed excitation

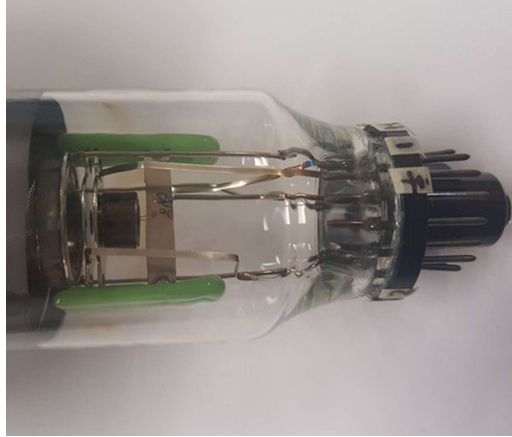


Figure 2.3: Picture of the electron gun in Vu1 light bulb

2.2 Design of the high voltage pulsed supply.

The pulse power supply is based on flyback topology [3,14,15]. This design has many advantages, such as simplicity and relatively easy implementation. It is used for low power applications between 1W to 100W, and it also has a low cost. The circuit has been designed, constructed, and implemented in a commercial light bulb provided by Vu1.

2.2.1 Flyback Transformers Power Supply.

The essential components for the flyback transformer are the converter, controller IC, RC Snubber, primary switching MOSFET, and secondary rectifier. The Flyback transformer power supply diagram is shown in Figure 2.4.

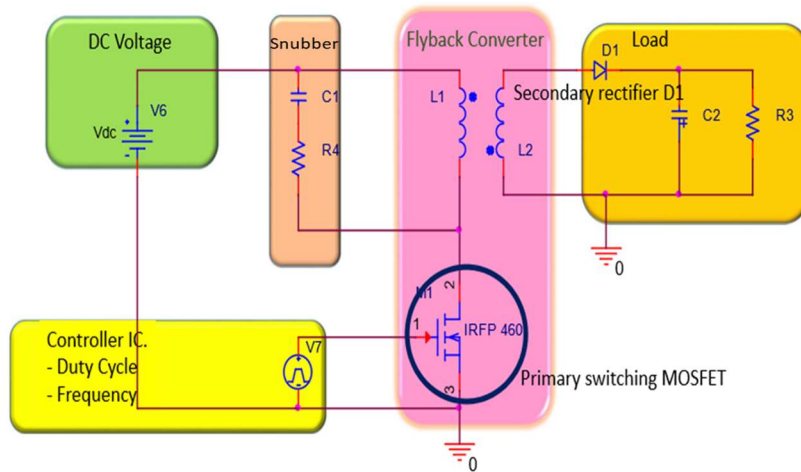


Figure 2.4: Diagram of the flyback transformer.

The flyback transformer operates when the IC controller emits a positive signal in $t_0 = 0$, producing the switch mode turned on, then, the current starts to rise linearly, this current goes by the primary winding of the transformer, and the magnetizing inductance is charged by the DC voltage source. Then, the controller emits no signal in $t = t_1$, the switch mode is turned off and the energy stored in the primary winding will be coupled to the secondary winding. This energy in the secondary will be transformed in a well-defined high voltage peak with a proper rectifier.

The flyback transformer can be designed for two modes, CCM (Continuous Conduction Mode) or DCM (Discontinuous Conduction Mode). In DCM, the energy stored in the core is delivered to the secondary winding during a Flyback period, and the primary current falls back to zero before the switch turns on again. For CCM, the energy stored in the primary winding is not completely transferred to the secondary, which means the Flyback current does not reach zero before the next switching cycle. The illustration describes the functioning of the DCM mode designed in Figure 2.5.

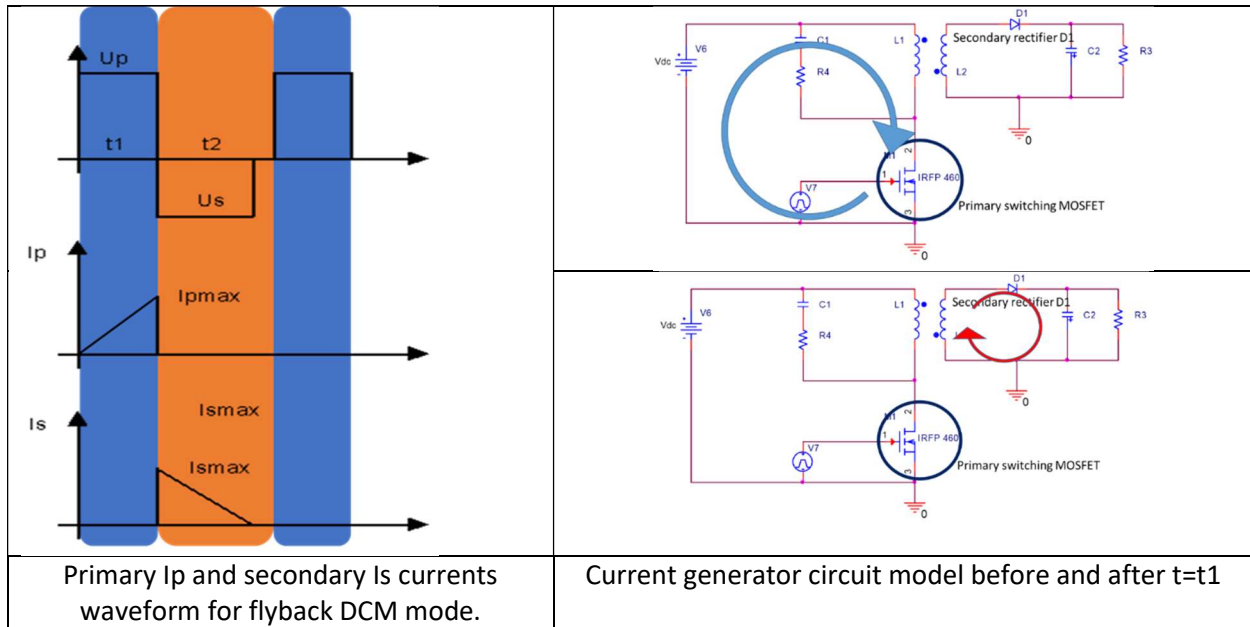


Figure 2.5: Flyback - switching cycle DCM Mode

To obtain the peak current in the primary winding side, the equation 2.1 is used [2].

$$I_{pp} = \Delta i_{Lm} = \frac{V_{DC}}{L_m} (t_1 - t_0) \quad \text{eq. 2.1}$$

Where the variables are represented as

L_m = Magnetizing inductance in primary.

I_{pp} = Peak current in primary.

Δi_{Lm} = Magnetizing inductance current.

Input power can be described with equation 2.2.

$$P_{in} = \frac{1}{2} (L_m) (I_{pp})^2 (f_{sw}) \quad \text{eq. 2.2}$$

Where f_{sw} is the frequency of the primary switching MOSFET.

The energy on the primary and secondary coil can be calculated by the following equations.

$$E_{pri} = \frac{1}{2} L_m I_m^2 \quad \text{eq. 2.3}$$

$$E_{sec} = \frac{1}{2} C_o V_o^2 \quad \text{eq. 2.4}$$

$$V_o = I_m \sqrt{\frac{L_m}{C_o}} \quad \text{eq. 2.5}$$

$$\left(\frac{dv}{dt}\right) = \frac{I_o}{C_o} = \frac{I_m}{nC_o} \quad \text{eq. 2.6}$$

2.2.2 Flyback converter.

The flyback transformer is an integrated transformer. It is a multi-winding coupled inductor constructed for high frequency and commonly used for high voltage output about 24kV. They are implemented in old televisions or CRT. In this specific case, the Toshiba 23236254 transformer flyback TFB4100AD is used; for this specific work, the primary winding must support around 0.2 amp and, the secondary winding should support a pulse of 1KV peak voltage. Figure 2.6 shows a picture and a schema of the input and output connectors of the flyback transformer.

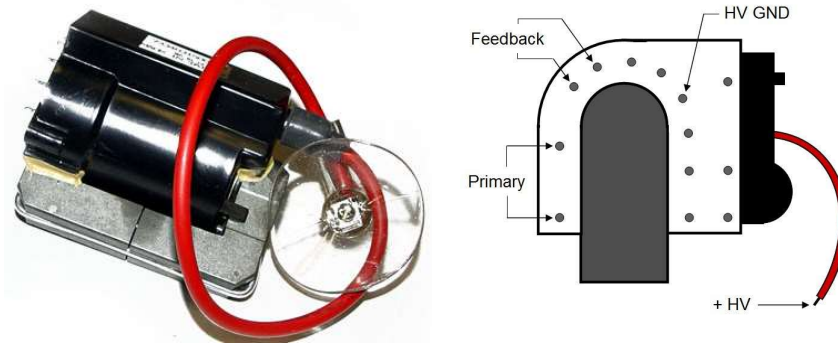


Figure 2.6: Flyback Transformer

2.2.3 IC controller

The main requirement for the IC controller is the frequency and duty cycle. The 555 timer IC shown in Figure 2.7 accomplishes the requirements.

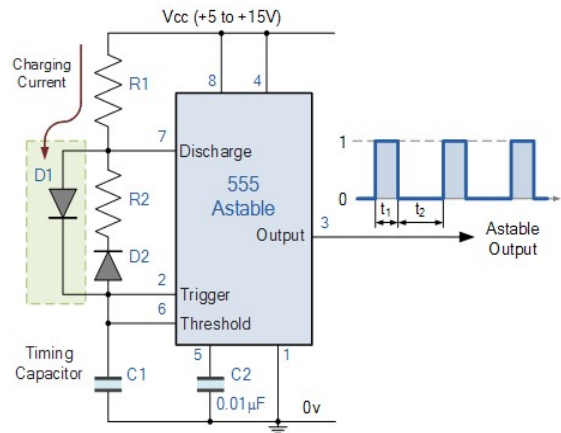


Figure 2.7: IC controller using diodes.

The equations 2.7 and 2.8 of the frequency f and Duty cycle DC describe and model the 555 timer IC.

$$f = \frac{\ln(2)}{(R_a + 2 * R_b) * C} \quad \text{eq. 2.7}$$

$$DC = \frac{R_b}{R_a + 2 * R_b} \quad \text{eq. 2.8}$$

2.2.4 Switching MOSFET

The output current in the MOS is determined at the control terminal and has nonideal parasites that lead to ringing waveforms, which produce that failure and noise levels higher than necessary.

Figure 2.9 shows the output signal in the switch mode without the RC snubber. This behavior is due to the turn-off of the power switch when it interrupts current through the leakage inductance of the transformer cause a voltage spike on the drain of the MOSFET.

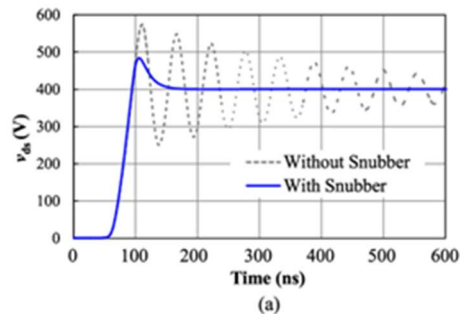


Figure 2.8: Turn-off of the power switch signal in the switch mode without the RC snubber

The inductance will then ring with stray capacitances in the circuit, producing large-amplitude high-frequency waveforms as shown in Figure 2.8. On the flyback primary, the measured leakage inductance rings with primary capacitances. Figure 2.9 shows the RC snubber used to suppress the problems mentioned before.

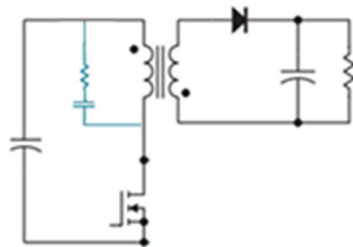


Figure 2.9: RC snubber circuit design

The parameters of the RC snubber can be obtained with the following procedure. First, the characteristic impedance of the resonant circuit is calculated by the equation 2.9

$$Z = 2\pi f_r L \quad \text{eq. 2.9}$$

Then, using $R=Z$ the resistor is calculated

$$R = 2\pi f_r L \quad \text{eq. 2.10}$$

The snubber capacitor is used to minimize dissipation at the switching frequency, while allowing the resistor to be effective at the ringing frequency.

$$C = \frac{1}{2\pi f_r R} \quad \text{eq. 2.11}$$

The dissipation is determined by the size of the snubber capacitor. The approximate dissipation is given by:

$$P = CV^2 f_s \quad \text{eq. 2.12}$$

2.3 Flyback Transformer Simulation

A model was simulated in top spice, and the answer can be shown in Figure 2.10. It is designed for a voltage of 1.2kV, the frequency is 300Hz, and a duty cycle is around 3%. Table 2.1. shows the passive and active components used in the simulation.

Table 2.1: List of active and passive components for flyback transformer simulation.

Passive and active elements	Values
C3	10n
MOSFET	IRFP460
R1	1.2k
R2	3k
R3	330

C1	1Uf
C2	0.01Uf
R5	0.33
C4	0.4Uf
TF Primary	12uh
TF Secondary	1.1h

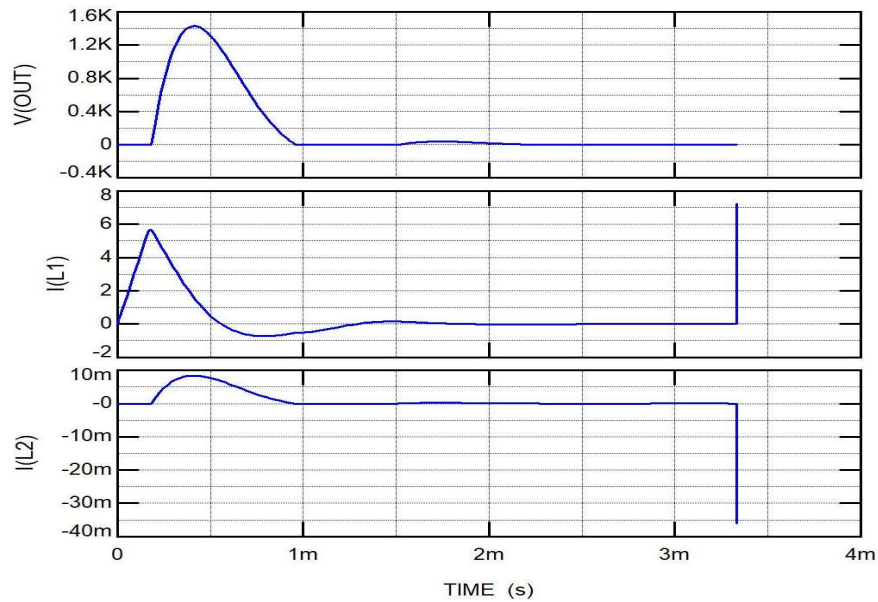
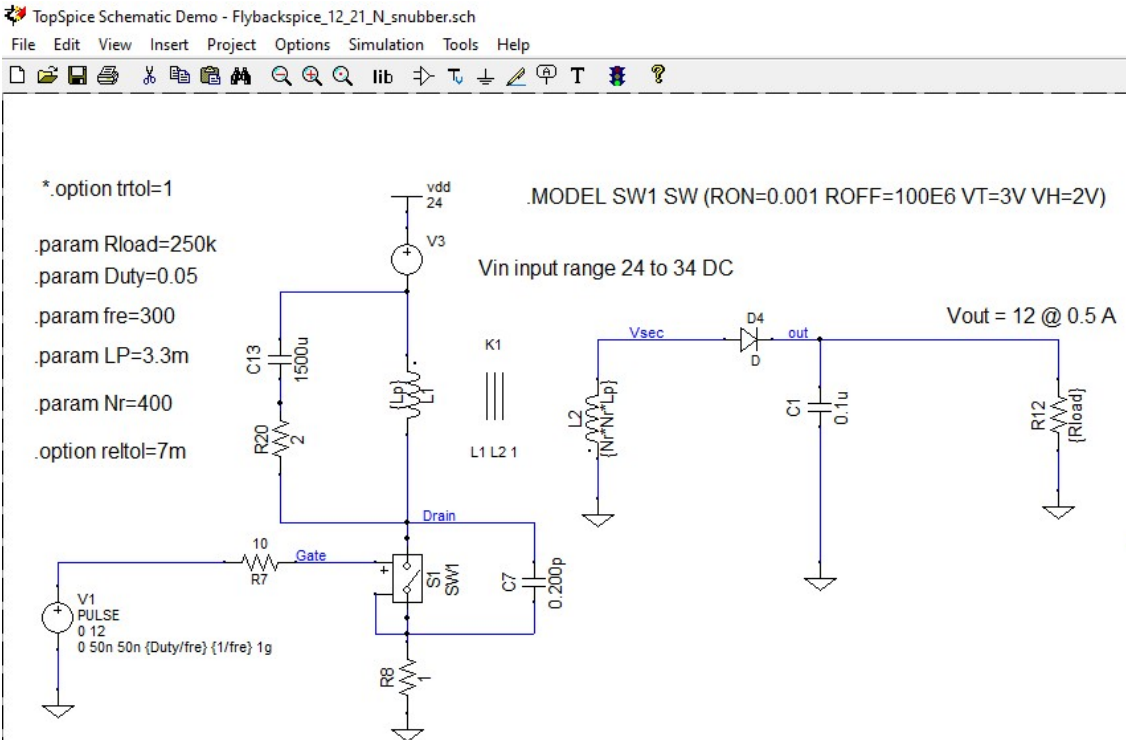


Figure 2.10: Circuit and results of pulsing power supply simulation, Top spice

In Figure 2.10. the $I(L1)$ represents the current in the primary winding, $I(L2)$ represent the current through the load, $V(out)$ represents the output voltage in the load, the FWHM is 476 us, which represents 14% of duty cycle and 300 Hz.

2.4 Flyback series connection

Implementing the flyback schematic shows 2.11, the maximum output voltage obtained is 1.4 kV at 300Hz with a duty cycle of 8%. One way to increase the output peak is using a series of flyback topologies. The topology uses N multiples flyback power sources, which can increase the output voltage in N times. The circuit is shown in Figure 2.11

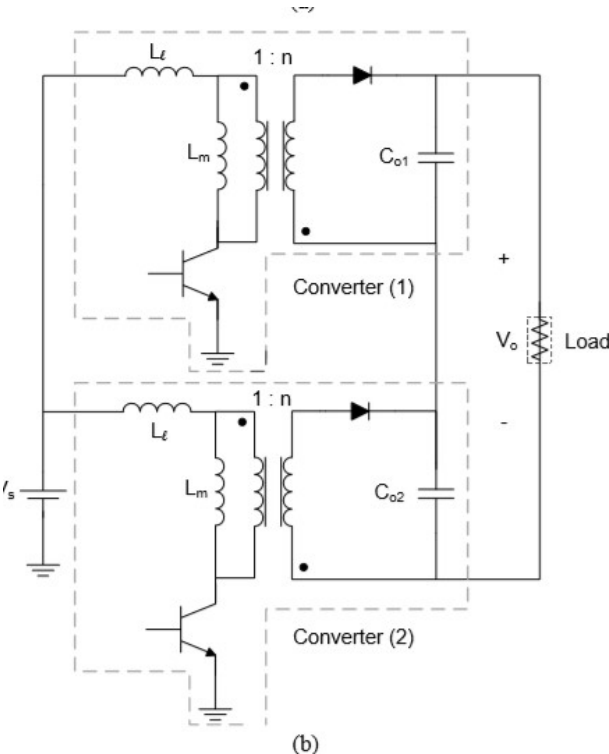


Figure 2.11: Flyback converter series connection.

The idea of series connections of the flyback modules is applied to the secondary side, while the primary sides are parallel. The output voltage magnitude and its rate of rising can be expressed as:

$$V_{o \text{ Series}} = \sqrt{2} I_m \sqrt{\frac{L_m}{C_{OS}}} \quad \text{eq. 2.13}$$

$$\left(\frac{dv}{dt}\right)_{\text{Series}} = \frac{I_o}{C_{OS}} \quad \text{eq. 2.14}$$

where C_{OS} is

$$C_{OS} = \frac{C_{O1} C_{O2}}{C_{O1} + C_{O2}} \quad \text{eq. 2.15}$$

The series module connection improves the output voltage level and rises time as the output capacitance decreases. Here the series modules are beneficial for both voltage levels and its rate of rising when $C_{OS} < C_O$.

$$V_{o \text{ Series}} = \sqrt{N} \frac{V_{in}}{\sqrt{L_m C_o}} D \cdot T \quad \text{eq. 2.16}$$

Usually, this adjustment is performed by limiting the current by selecting suitable duty cycle (D). But it should be calculated in a way that $I_m < I_{sat}$, where I_{sat} is the current saturation level of the transformer.

The reflected voltage across the switch for N-series module can be rewritten as below:

$$(v_{switc})_{max} = V_s + \frac{1}{N_n} v_{o \text{ max}} \quad \text{eq. 2.17}$$

Chapter 3

Experimental Results and Analysis

In this chapter, the performance of the high pulsed voltage supply is measured and implemented in the light bulbs provided by Vu1. In addition, the DC driving method for phosphor lamp is tested and compared with the pulsed method regarding temperature and luminance. All the experiences were done in the Vacuum Microelectronic Laboratory at UC Davis.

3.1 Pulsed Voltage Supply

The performance of the pulsed voltage described in Chapter 2 is implemented with multiples series flybacks. Five Flyback transformers implement the final flyback model with $180\mu\text{H}$ and $2\mu\text{H}$ as magnetic and primary windings, five 3kV diodes, five 10pf capacitors, and a 200k resistor. The IC controller is implemented with Texas Instruments NE555P. The output voltages can be adjusted for the required level, whether by V_{in} , capacitors, frequency, or duty cycle. The frequency and duty cycle values for the controller used for this work were between 90 and 1k Hz and between 1% and 10 %, respectively. The power data was collected using DS1054Z Rigol oscilloscope and plotted by Matlab. The characteristics of the three pulses used are shown in Figure 3.1. The duty cycle of the output voltage on the flyback is calculated by the Full Wave Half Maximum (FWHM).

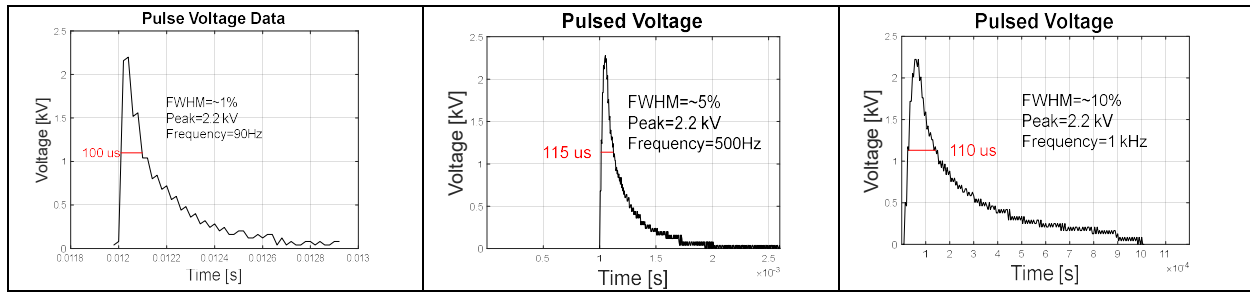


Figure 3.1. Flyback Output Voltage

3.2 Pulsed and DC excitation driving the Vu1 light bulb.

In this section, the performance of the DC were the pulsed excitation are measured in the Vu1 light bulb, and the results are shown using MATLAB 2020a software.

A light bulb is used to test the DC voltage and the SPELLMAN DC Power Source provide the high DC voltage. The Konica Minolta Meter LS-100 read luminance at 1m from the light bulb, which was placed in front of the center of the light bulb's glass. The temperature is read by an Infrared temperature sensor made by OMEGA.

3.2.1 Experimental results by using pulsed voltage excitation.

The results of the temperature and luminance variables are shown in Figure 3.3. The schematic for the set-up is shown in Figure 2.2. and the values of voltage and current of the set-up are shown in Table 3.1. Figure 3.2 shows the stabilization time of Vu1 light bulb for pulsed excitation.

Table 3.1: Values applied to the Vu1 light Bulb.

VG1[V]	VG2[V]	VG3[V]	Heater [A]	Heater [V]	V_anode	I_anode
0	Pulse	10	0.82	2V	15K	350 us

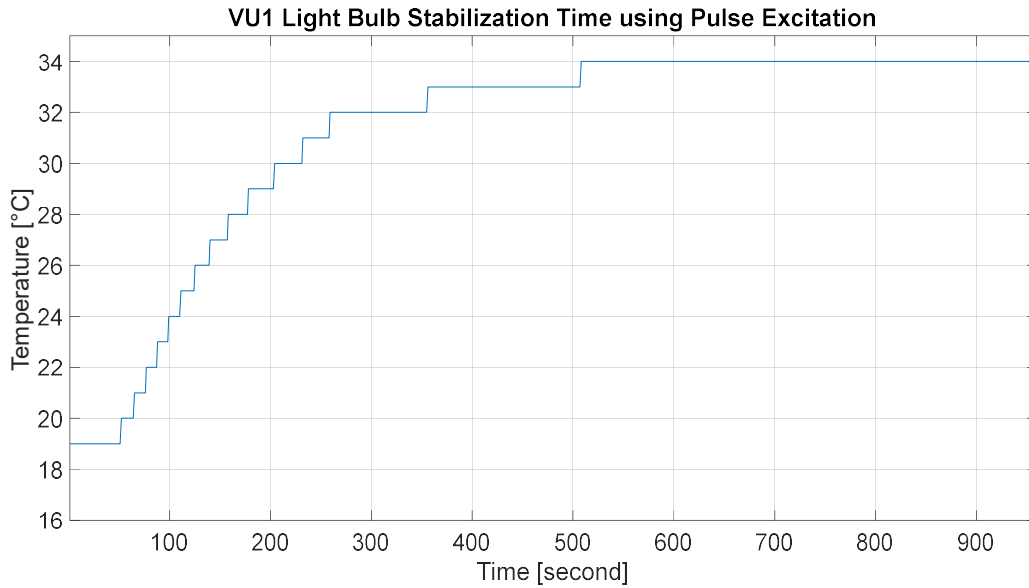


Figure 3.2: Stabilization time of Vu1 light source by using pulse excitation.

In this experiment, the Vu1 light bulb is tested with a pulsed excitation on the electron gun and a DC voltage of 10KV, 12KV, and 15kV. Temperature, luminance, voltage, and the anode current measurements were collected and plotted by using MATLAB and are shown in Figure 3.3, Figure 3.4, Figure 3.5, Figure 3.6.

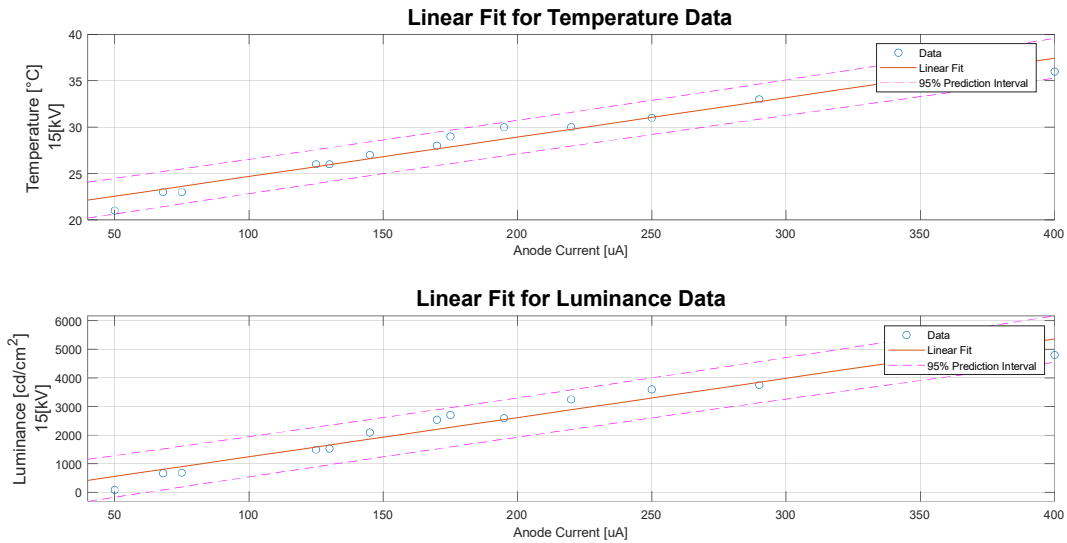


Figure 3.3: Luminance and temperature for different anode current and accelerating voltage of 15kV DC.

Figure 3.3 shows the data collected in blue circles. The red line is the linear fit curve calculated, using the functions polyfit and polyval from MATLAB.

The polyfit is a polynomial curve fitting which returns the coefficients for a polynomial $p(x)$ of degree n that is a best fit (in a least-squares sense) for the data in y . The coefficients in p are in descending powers, and the length of p is $n+1$.

$$P(x)=p_1x^n+p_2x^{n-1}+\dots+p_nx+p_{n+1}.$$

As seen in the graph the linear model includes an estimate of a 95% prediction interval. It is created by a few vectors of sample data points (x,y) and it specifies the error estimation structure as the third input so that polyval calculates an estimate of the standard error. The standard error estimate is returned in the delta. Then, the 95% prediction interval is calculated by $y\pm 2\Delta$. All the following graphs will include only polynomial curve fitting to express the difference between the data collected.

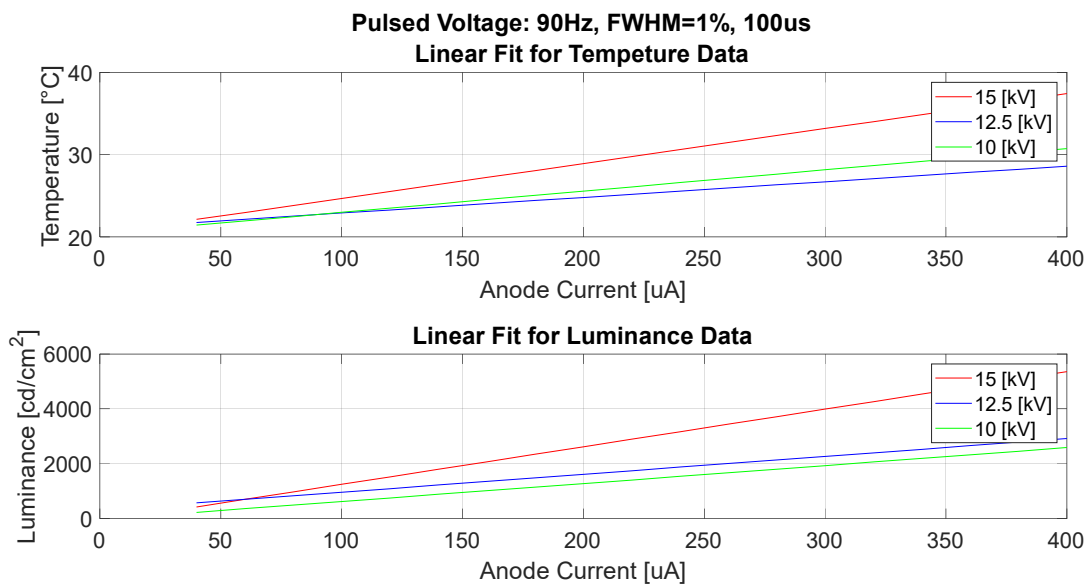


Figure 3.4: Data collected using pulse excitation with a frequency of 90 Hz.

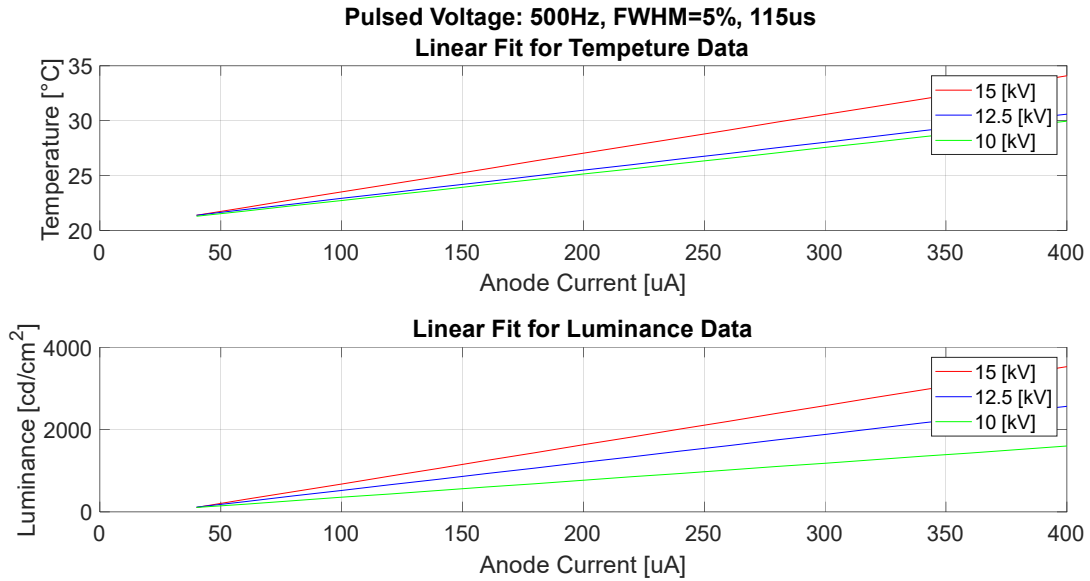


Figure 3.5: Data collected using pulse excitation with a frequency of 500Hz.

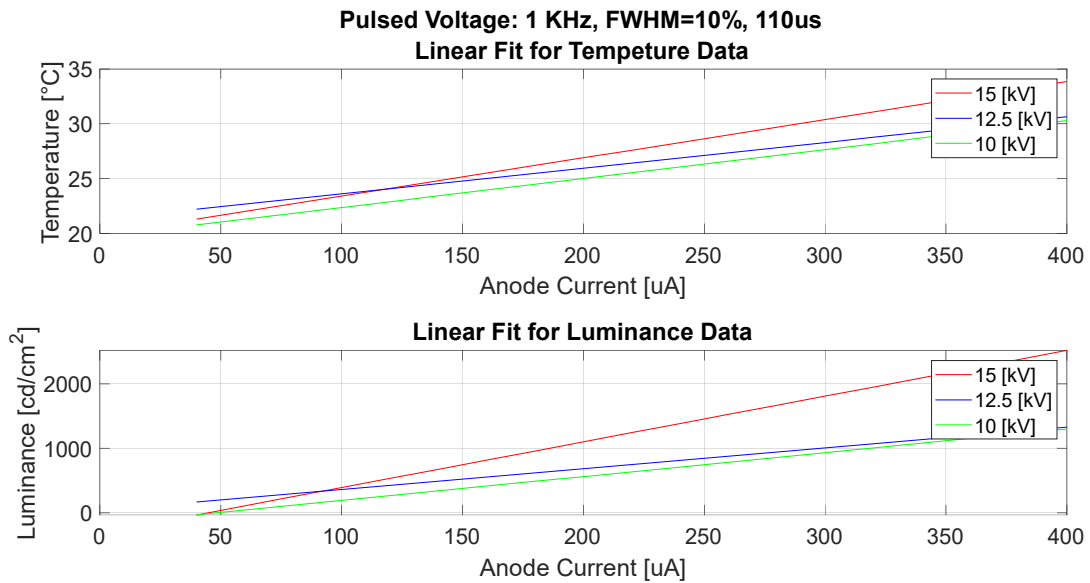


Figure 3.6: Data collected by using pulse excitation with a frequency of 1 kHz.

Figure 3.4, Figure 3.5, Figure 3.6 shows the temperature and luminance linear fit for different current densities and accelerating voltages. For all the experiments, the temperature and luminance increase by increasing accelerating voltage which is due to the energy increment

in the electron that impact the phosphor material generating more secondary emission and temperature.

For all experiments, the temperature and the luminance increase by increasing the anode current.

3.2.2 Experimental results by using DC voltage excitation.

The schematic proposed to drive the cathodoluminescent phosphor lamp is shown in Figure 2.1. Figure 3.7 shows the stabilization time for the Vu1 light bulb with the parameters described in the Table 3.2. VDC and IDC correspond to the values for the accelerating voltage.

Table 3.2: Values applied to the Vu1 light Bulb.

VG1[V]	VG2[V]	VG3[V]	Heater [A]	Heater [V]	VDC [KV]	IDC [mA]
0	100	100	1.1	2	15k	0.229

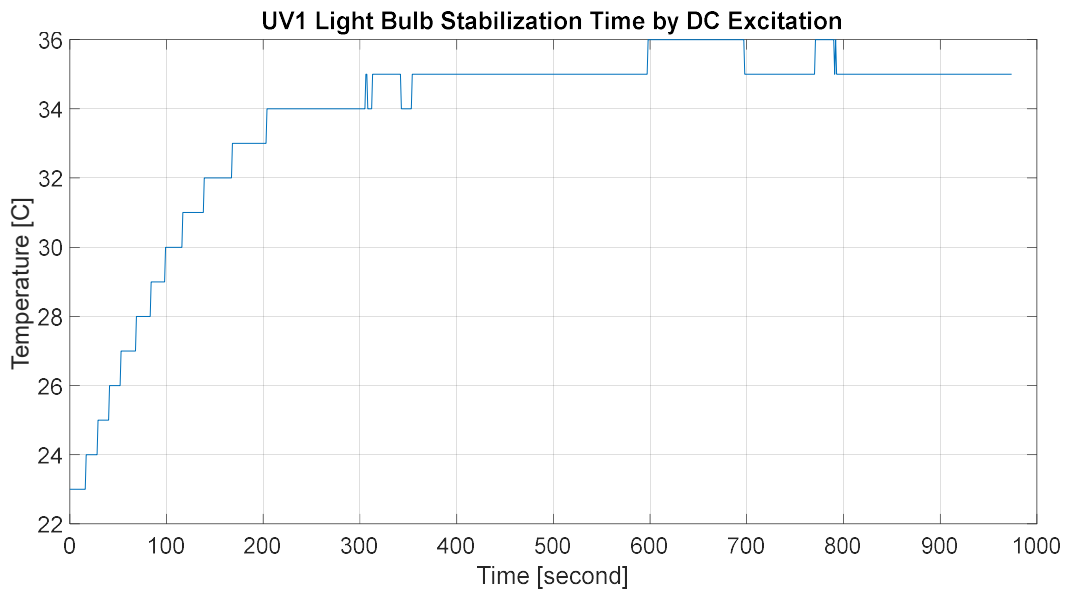


Figure 3.7: Stabilization time of the Vu1 light source by using DC excitation.

In this experiment, the Vu1 light bulb is tested using DC accelerating voltage of 10kV, 12.5kV and 15kV. The current density was also incremented by increasing the voltage connected to the heater. Temperature, luminance, voltage, and the anode current

measurements were collected and plotted by using multimeters, oscilloscope and MATLAB. The parameters for the electron gun are shown in Table 3.3. and the results are shown in subplots in Figure 3.8

Table 3.3: Voltages applied to electron gun for DC excitation.

Vg1	Vg2	Vg3	Current Heater [A]	Voltage Heater [V]
9.33	0	10	1.1	2

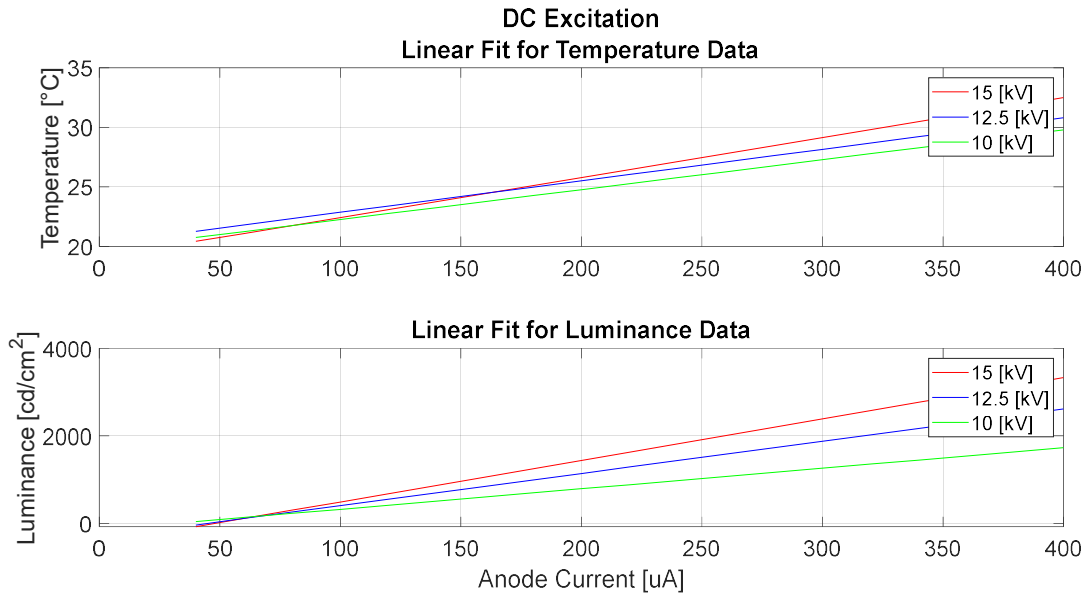


Figure 3.8: Data collected by using DC excitation.

For all experiments, the temperature and the luminance increase by increasing the anode current.

3.3 Comparison

3.3.1 Comparison of the results by using different Pulsed excitation.

In this section, the collected data of pulsed excitations are compared and analyzed.

Figure 3.9 and Figure 3.10 show the linear fit of the data sorted by accelerating voltage.

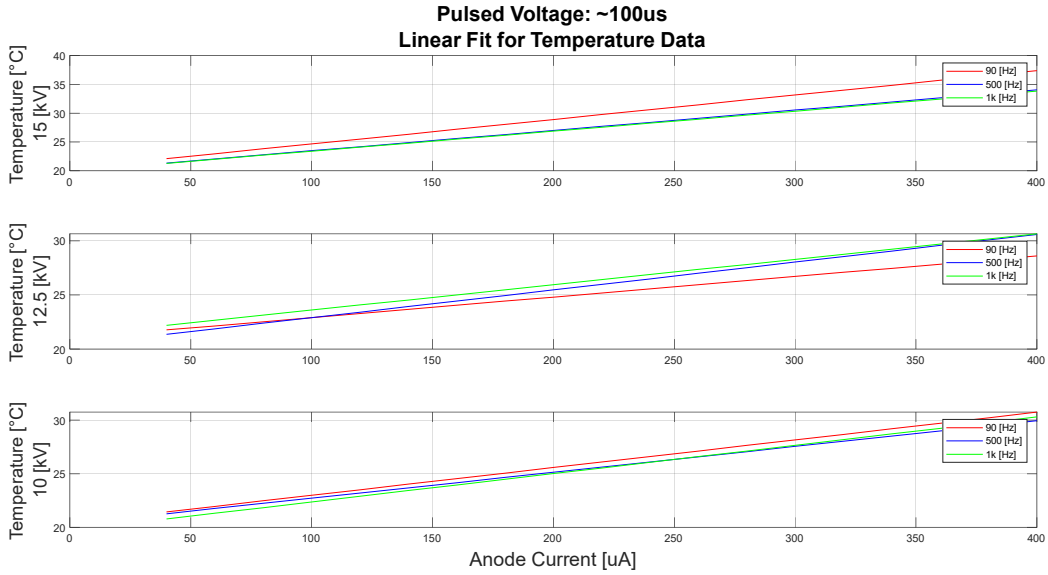


Figure 3.9: Vu1 Temperature results by using different Pulsed excitations.

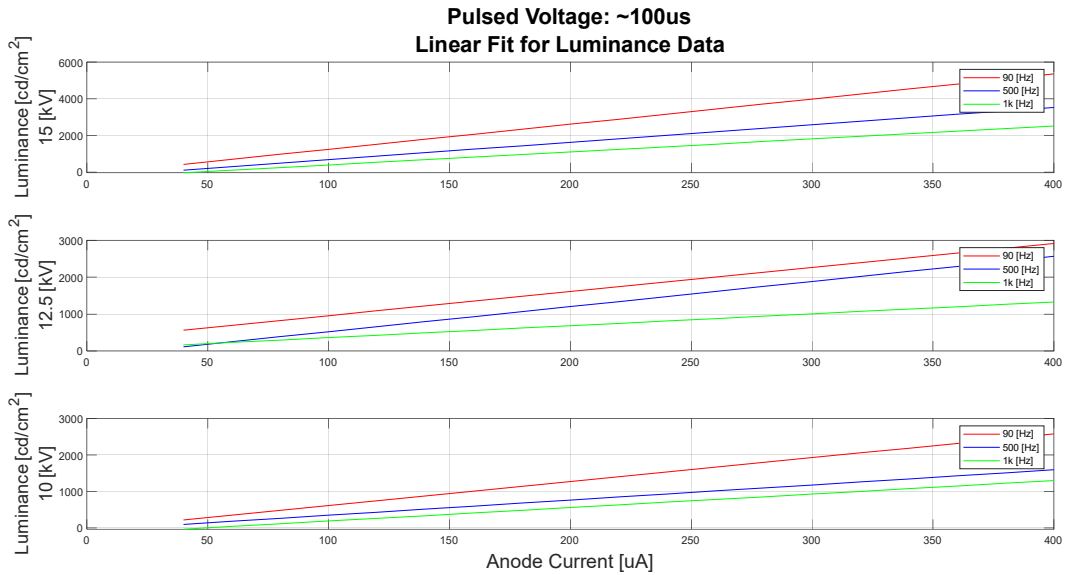


Figure 3.10: Vu1 luminance results by using different Pulsed excitations.

Figure 3.10, shows that there is no clear difference in term of temperature at different frequencies. In Figure 3.11, an increment in luminance by decreasing the frequency on the

pulsed excitation can be seen, which means that at lower frequencies pulsed excitation are producing more light.

Considering that the time “on” is practically the same for all the pulses but the time ‘off’ is higher for the lower frequencies. the increment can be due to the reduction in the current density or the number of electrons penetrating the phosphor material during a cycle.

3.3.2 Comparison between different Pulsed and DC excitations.

Figure 3.11 and Figure 3.12 show the comparison between the pulsed excitation at 90Hz, 500Hz, 1k Hz, and the direct current voltage excitation.

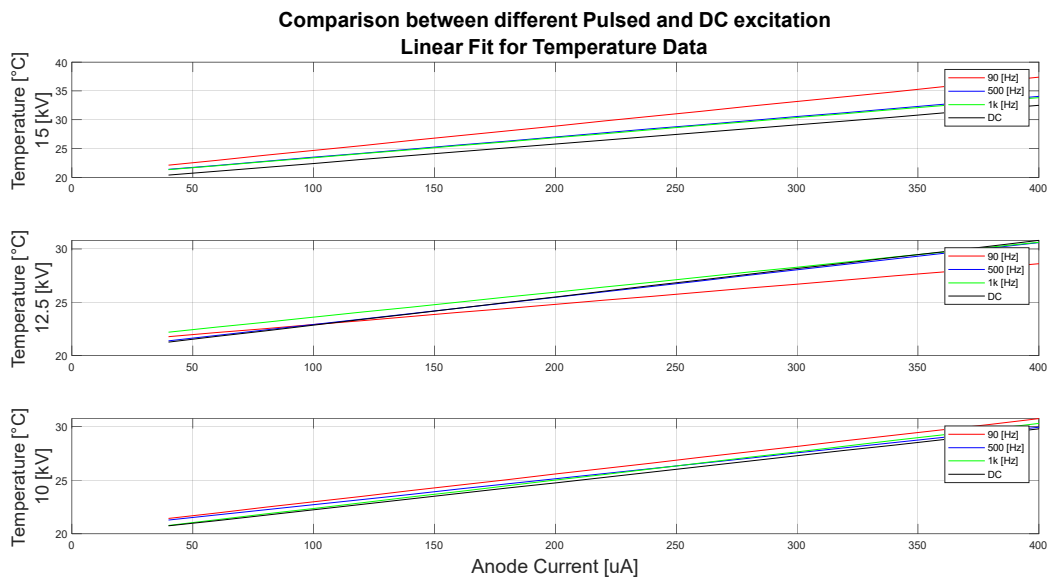


Figure 3.11: VU1 Temperature results using different Pulsed and Direct Current excitation.

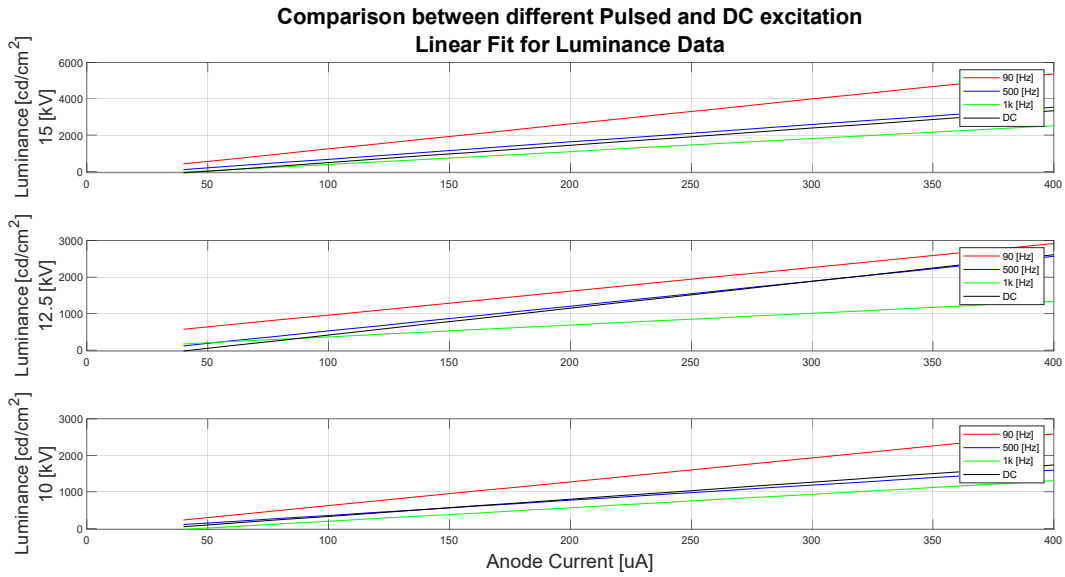


Figure 3.12: VU1 Luminance results using different Pulsed and Direct Current excitation.

Figure 3.11 and Figure 3.12 show that at the same anode current for different frequencies, decreasing the frequencies increase the light. It can also be seen that the temperature is strongly related to at the anode current and accelerating voltage.

Figure 3.13 shows the ratio calculated by dividing the luminance produced by pulsed excitation divided by the luminance produced by DC excitation.

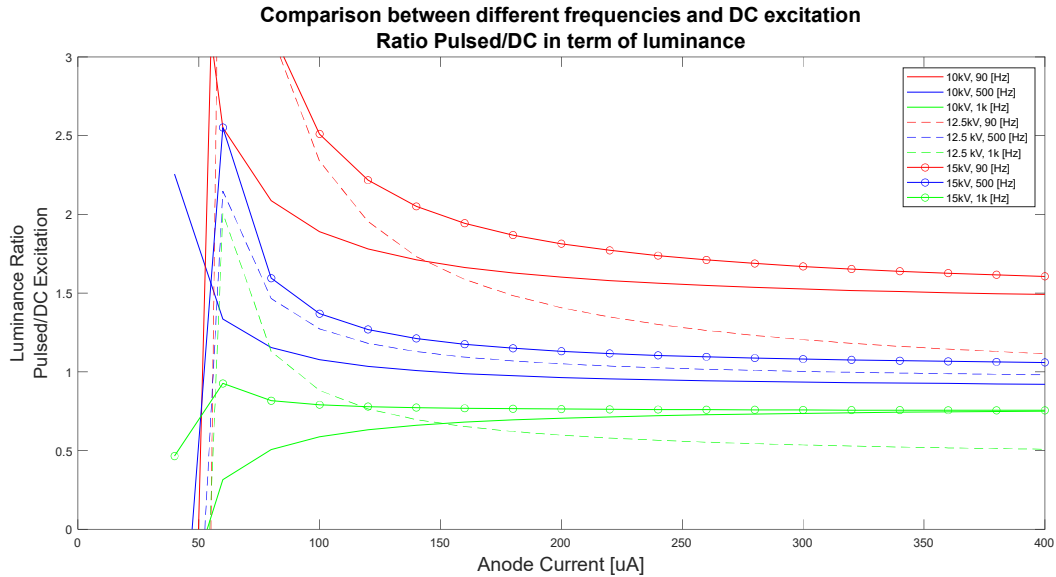


Figure 3.13: VU1 Luminance results ratio of Pulsed/DC excitation.

In Figure 3.13, The increment of luminance at lower frequency can be due to the reduction of the electron dose, which is associated with the efficiency of the material to produce light as shown in Figure 1.9.

Another explanation for the increment of luminance by lowering the frequency of the pulsed excitation, is to consider that the increment of the rest time will decrease the average temperature in the material during a cycle reducing the action of thermal killers in terms of “bypassing”, which is a type of killer that captures free carriers in competition with luminescent centers during the diffusion process of the free carriers, allowing them to recombine non radiatively.

4 Conclusion and Future Work

The flyback was constructed successfully by non-expensive cost and simple design, it also accomplished the values of 7kV with FWHM lower than 1%, and the output voltage, frequency, and duty cycle are easily adjusted for the required level whether by DC input voltage, output capacitors, the input frequency, or duty cycle of the IC controller. The Flyback pulsed power supply has successfully implemented on the Vu1 phosphor light source.

The implementation of pulsed excitation on the phosphor lamp source showed a better performance in terms of luminance and temperature having a maximum improvement around 170% when comparing 90Hz and direct current excitation at 15 kV of accelerating voltage. In this work, more luminance from the cathodoluminescence method is produced by reducing temperature. As a result, the lifetime of phosphor light bulbs was extended using pulsed excitation. Additionally, the experiments performed demonstrated that the luminance is higher by using pulsed excitation rather than direct current excitation, concluding that the efficiency of the phosphor lamp was increased.

In this work, the high voltage pulse was applied to the electron gun. However, a higher voltage pulse can be applied as accelerating voltage between anode and cathode. The future outlook should consider the excitation of high pulse with dc offset, which could be created by using the flyback transformer on the Continuous Conduction Mode CCM. The dc offset should provide a minimum excitation to generate a low electron dose to crash the phosphor layer. It should be low enough to prevent electron accumulation and keep a fluid path between the

phosphor and the aluminum layer. The DC voltage should maintain the light on if the phosphor material does not have enough persistence. Then, the pulse can be super positioned to increase the electron's energy but low enough "on" time to reduce the electron accumulation in the phosphor layer.

References

- [1] "U.S. Energy Information Administration (EIA)", accessed 08/18/2021.
Available: <https://www.eia.gov/tools/faqs/faq.php?id=99&t=3>
- [2] R. Haitz, J. Tsao. "Solid-state lighting: 'The case', 10 years after and future prospects", *Physics Status Solidi*. No. 1,17-29, 2011, doi:10.1002/pssa.201026349
- [3] C. Lin, M. Hung, C. Ho and C. Wang, "High voltage pulse power supply for driving tubular field emission lamp based on flyback topology," *TENCON 2011 - 2011 IEEE Region 10 Conference*, 2011, pp. 898-902, doi: 10.1109/TENCON.2011.6129240.
- [4] M. Cao, R. Chacon, and C. Hunt, "A Field Emission Light Source Using a Reticulated Vitreous Carbon (RVC) Cathode and Cathodoluminescent Phosphors," *J. Display Technol.* 7, pp:467-472 (2011)
doi: 10.1109/JDT.2011.211615
- [5] C. Hunt, and S. Blackstone, "HIGH-QUALITY, ENERGY-EFFICIENT AND AFFORDABLE LIGHT SOURCE USING CATHODOLUMINESCENT PHOSPHORS" (Invited", *Light Sources 2012*, R. Devonshire and G. Zissis, Ed.s, Lighting Research Center, Tory, NY, p. 395-396, (2012). 144
Available: <https://www.ece.ucdavis.edu/huntgroup/home/publications>
- [6] G. Garlick, "The kinetics and efficiency of cathodoluminescence", *British Journal of Applied Physics*, 2002, Vol:13, pp:541, doi: 10.1088/0508-3443/13/11/306
- [7] T. Hase, T. Kano, E. Nakazawa, and H. Yamamoto, "Phosphor materials for cathode-ray tubes", *Advances in electronics and electron physics*, 1990, vol: 79, pp:271-373
- [8] M. Itoh, and L. Ozawa, "Cathodoluminescent phosphors", *The Royal Society of Chemistry* 2006, 2006, pp:12-42, doi: 10.1039/B417154N
- [9] C. Schwarz, L. Chernyak, and E. Flitsiyan, "Cathodoluminescence Studies of Electron Injection Effects in Wide-Band-Gap Semiconductors", *Cathodoluminescence*, Naoki Yamamoto, doi: 10.5772/33655.
Available: <https://www.intechopen.com/chapters/34034>
- [10] W. T. Dyll. MASSACHUSETTS INSTITUTE OF TECHNOLOGY Research Laboratory of Electronics, A Study of the persistence characteristics of various cathode ray tube phosphors, 1948, Accessed: Aug. 17, 2021, Available: <https://dspace.mit.edu/bitstream/handle/1721.1/4992/RLE-TR-056-04706923.pdf>
- [11] N. Chubun, A. Chakhovskoi, and C. Hunt "Efficiency of cathodoluminescent phosphors for a field-emission light source application", *Journal of Vacuum Science & Technology B: Microelectronics and Nanometer Structures Processing, Measurement, and Phenomena* 21, 2003, 1618,
doi:10.1116/1.1587134
- [12] P. Davari, "High Frequency High Power Converters for Industrial Applications", PH.D. dissertation, Electrical Engineering and Computer Science, University of Technology Queensland, Queensland, Australia, 2013. [Online]. Available: https://eprints.qut.edu.au/62896/1/Pooya_Davari_Thesis.pdf

[13] P. Moleme, S.Pitale, H. Swart, and O. Ntwaeaborwa, "Investigation of ageing characteristics and identification of surface chemical changes on SrGa₂S₄:Ce³⁺ display phosphor under electron beam bombardment", 2012, Physica B: Condensed Matter, Volume 407, Issue 10, 15, pp:1645-1648, doi:10.1016/j.physb.2011.09.107

[14] P. Davari, F. Zare, A. Ghosh and H. Akiyama, "High-Voltage Modular Power Supply Using Parallel and Series Configurations of Flyback Converter for Pulsed Power Applications," in IEEE Transactions on Plasma Science, 2012, vol. 40, no. 10, pp. 2578-2587, doi: 10.1109/TPS.2012.2199999.

[15] C. Lin, C. Wang, M. Hung and C. Ho, "High voltage driving circuit with negative pulse feature for tubular field emission lamp," 2010 5th IEEE Conference on Industrial Electronics and Applications, 2010, pp. 1118-1123, doi: 10.1109/ICIEA.2010.5515846.